Particle Misidentification in the Invariant Mass Spectrum of the Delta Resonance

Alexander Grounds
Principal Investigator: Christina Markert

May 3, 2013

Abstract

The quark-gluon plasma is a new phase of matter and is the focus of much research in particle physics today. One of the main purposes of the famous Large Hadron Collider (LHC) at CERN is to create quark-gluon plasma by colliding lead nuclei at high energies. The plasma can only exist for extremely short amounts of time, so our only method of investigating it is to analyze the particles it produces. This is one of the goals of A Large Ion Collider Experiment(ALICE) and the construction of the ALICE detectors at the LHC. Of particular importance are so-called resonance particles. Like the quark-gluon plasma, these particles only live for very short amounts of time before decaying. Therefore, they can be created and even re-created while the plasma exists. For this reason, they are extremely important to our analysis of the quark-gluon plasma. However, since they are so short-lived, we cannot directly see these resonance particles either. Rather, we look at the longer-lived particles which they decay into. We determine facts about the resonances from the information we have about their decay products.

However, identifying these decay products can be difficult as well, especially in high-energy experiments such as those in ALICE. It is often the case that we think that a particle is a pion, for instance, when indeed it was a proton. This is called a misidentification. By misidentifying decay products, we then misidentify the particle from which those products decayed. To account for this phenomenon, we simulate particle misidentification. The simulation gives us expectations for the shape of distributions of misidentified particles. Knowing the shape, we can then attempt to locate these distributions in experimental data and subtract them out to produce a cleaner distribution of our resonance particle.

In this paper, we analyze the invariant mass distribution of the Δ^0 resonance. We look at four other particles which can by misidentified as the Δ^0 and analyze their misidentified invariant mass distributions. We then investigate the dependence of these distributions upon the particle's momentum. The analysis gives us information about when it is possible to find a misidentified particle's distribution inside an experimental distribution of the Δ^0 mass and what shape we should expect the misidentified distribution to take. This analysis will be useful for further studies of the Δ^0 in high-energy collisions.

Contents

1 Introduction

Particle physics is the study of the most basic units of matter — particles. These are the objects which make up everything we see around us, from the bacteria in our homes to the galaxies that surround us. Everything in the universe is composed of particles. Thus, the field of particle physics seeks to understand the physical laws which govern our universe at their most fundamental level.

One of the most fundamental topics of all is the study of the forces of nature. These interactions govern our entire universe. In particular, it is the strong force which rules the domain of hadronic physics. It determines the interaction of the quarks which make up all hadrons, such as protons and neutrons, and is often the force responsible for the interaction of hadrons with other hadrons. The theory of the strong interaction between particles is known as quantum chromodynamics (QCD). In this theory, the strong force between quarks is mediated by exchanging particles called gluons. The theory is one of the most important topics in theoretical physics today.

1.1 The Quark-Gluon Plasma

Between individual quarks, the strong interaction is an attractive force which acts like a spring [1]. When quarks are further away from one another, the force is greater between them, and when the quarks are close together, the force is very weak. Compared to other interactions, this force is quite strong as its name would suggest, so quarks bind together very tightly. These bound states are what we know as hadrons, composite particles made of quarks, such as the proton and the neutron among many others. Under ordinary circumstances, a quark cannot leave its hadron unless acted on by an outside force. For instance, we could collide two hadrons, A and B, in a scattering experiment. In so doing, one of the quarks of A might get very close to one of the quarks of B, resulting in quark-quark scattering and knocking one of the quarks out of its hadron. Even in this case, the energy of the strong interaction between the free quark and the quarks of its original hadron is great enough to produce a quark-antiquark pair. The quark and antiquark then combine with the other quarks to form new hadrons, as discussed below (see Figure 2). Thus, the quark which was "freed" by the interaction is immediately reconfined to a hadron.

Despite this strict description of the strong interaction between quarks, if we compress and heat a system of quarks enough, they can enter a new state of matter known as the quark-gluon plasma (QGP) [2]. When this happens, quarks are no longer restricted to stay within hadrons. Rather, they move more freely, without binding to other quarks. Experimentally, we create QGP by colliding heavy ions together at high energies. The QGP is the state of matter thought to have existed shortly after the Big Bang,

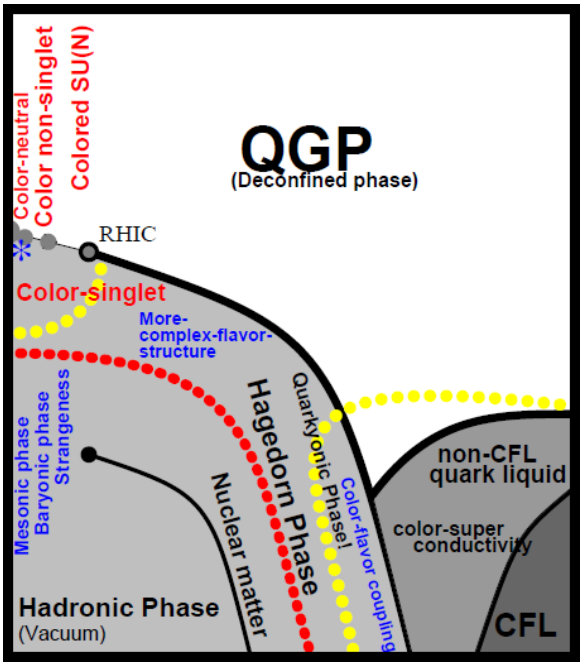

Figure 1: A Phase Diagram of the Transition from Hadronic Matter to QGP [4].

so by making QGP in the lab, we are creating "little Bangs" and studying the early universe.

The QGP is a state of matter in the same way that solids, liquids, gases and plasmas are states of matter. Thus, there is a phase transition between QGP and hadronic matter, i.e. ordinary matter in which quarks are confined to hadrons (see Figure 1) [4]. In addition, in a heavy ion collision, produced particles fly away from the point of collision in all directions. Thus, the QGP expands, dropping in temperature as it does so. Because the plasma must be very high in temperature to exist (as you can see in Figure 1), this expansion limits the QGP lifetime to only a few fm/c where c is the speed of light. In other words, the lifetime of the QGP is on the order of 10^{-23} seconds [3]. This is an extremely short lifetime. Indeed, it is too short for us to observe directly. Rather, we examine the QGP by observing the particles which it produces.

The strong interaction has charges associated to it, much like electric charge is associated with the electromagnetic interaction. Unlike the electromagnetic interaction, however, the strong force has three types of charge. These are referred to as color charges and are labeled red, green and blue. Having three types of charge, the theory of the strong interaction (QCD) is based on the matrix group SU(3). While we will not go into this description in detail in this paper, it is worth noting that the SU(3) algebra gives us two ways for colored quarks to form color-neutral bound states:

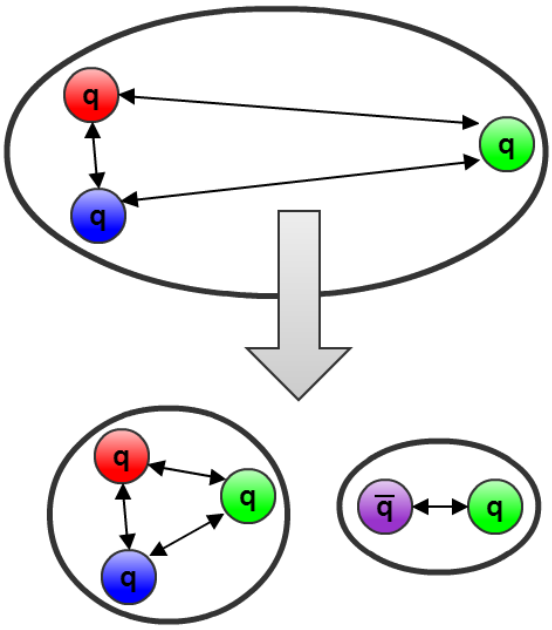

Figure 2: A hadron produces a quark-antiquark pair.

Three quarks, one of each color, may bind together and form a color-neutral hadron (these are called baryons) or a quark (with red color, for instance) may bind with an antiquark (with antired color in this case) [5].

When the strong interaction is given enough energy, it is capable of converting this energy into mass and producing new particles. It does this by creating quark-antiquark pairs, as shown in Figure 2. As the green quark is pulled away from the red and blue quarks, the strong force pulls harder on the quarks. Finally, when the interaction is strong enough, it has enough energy to produce a green quark and an antigreen antiquark. Thus, a hadron has been created. This same process occurs in the QGP. The plasma has sufficient energy to produce many quark-antiquark pairs. Then, as the plasma expands and cools, these quarks and antiquarks combine into many different particles. This process is called the particle production of the QGP. A single heavy ion collision may produce as many as 10,000 particles via the QGP, from only about 400 nucleons in the original nuclei.

1.2 The Δ Resonances

One particle of interest is the family of $\Delta(1232)$ resonances. (Note that the number in parentheses is the mass of the particle in MeV/c^2. This is common notation for resonance particles.) The resonances are baryons composed of up and down quarks, just as the nucleons, i.e. protons and

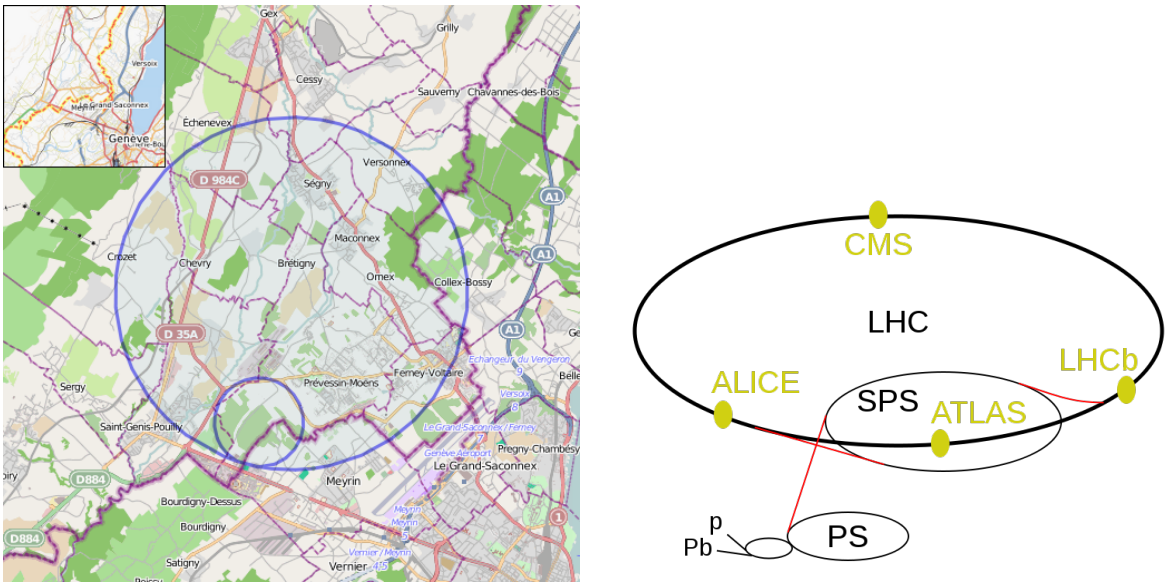

Figure 3: The LHC Location and Schematic

neutrons, are [6]. While the proton and neutron have an isospin of 1/2, however, the Δ resonances have an isospin of 3/2. By the rules of quantum angular momentum, this permits four I_3 states in the family, and hence four Δ particles. In particular, the Δ^0 is the bound state of two down quarks and an up quark, and it is the particle of interest in this paper.

The Δ^0 was first discovered in 1951 at the Chicago cyclotron [7]. Physicists there were examining the interaction between pions and nucleons when they found an increase in the interaction cross section between pions and nucleons near 180 MeV pion beam energy. This phenomenon of increase cross section near a particular energy was referred to as a resonance in the cross section, hence the name resonance for high-mass particles like the Δ^0. Since that time, the Δ^0 and its relatives have been studied in detail in many different experiments. Its quantum numbers are all known, its mass and width are known to good precision, and its decay channels have been well-explored.

One useful facet of the Δ^0 is its extremely short lifetime of about 5.6×10^{-24} seconds [6]. Being so short-lived, it can be produced in the QGP, decay in the QGP, and be produced again (i.e. regenerated) in the QGP, all in a single collision. Therefore, the Δ^0 is affected by the QGP in a very direct way compared to other, longer lived particles. Thus, any distributions we measure about the Δ^0 may be changed due to the interaction of the particle with the QGP. For this reason, the Δ^0 is an extremely important particle to examine in any QGP experiment.

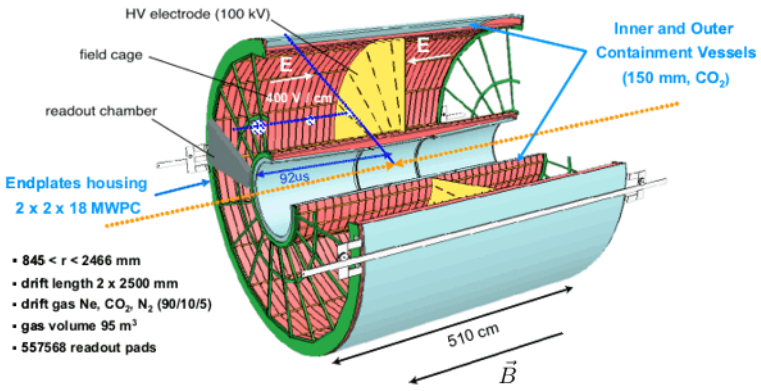

Figure 4: The ALICE Time Projection Chamber [8]

1.3 ALICE

A Large Ion Collider Experiment (ALICE) is the name of the experiment studying the QGP at the European Organization for Nuclear Research (CERN). It makes use of the world's highest-energy particle accelerator, the Large Hadron Collider (LHC). The LHC is the massive, stretching 27 kilometers in circumference, as shown in Figure 3. In order to bring the colliding particles up to the maximum energies of the LHC, other accelerators are used to speed the particles up before they enter the LHC. These are shown in the schematic in Figure 3.

1.3.1 The Time Projection Chamber

The primary detector used by ALICE for momentum measurements and particle identification is the Time Projection Chamber (TPC), shown in Figure 4 [8]. The TPC is a cylindrical detector filled with gas. When a charged particle travels through the gas, it knocks electrons free of the gas particles. Electric and a magnetic fields are applied parallel to the length of the tube, so free electrons drift towards the ends of the tube. These electrons travel parallel to the magnetic field, so their trajectories are not affected by the magnetic field, but rather they fly straight down the length of the tube into its ends. In addition, the air molecules provide resistance to the electrons' motion, balancing the force from the electric field, so the electrons drift at a constant speed in the gas chamber.

At the ends of the tube there are grids of Multi-Wire Proportional Chambers (MWPCs). These chambers consist of anode wires and cathode segmented pads. The free electrons move towards the anode wires and produce a readout signal on the cathode pads. Since the pads are segmented, this gives specific information about the position at which the electron hit the

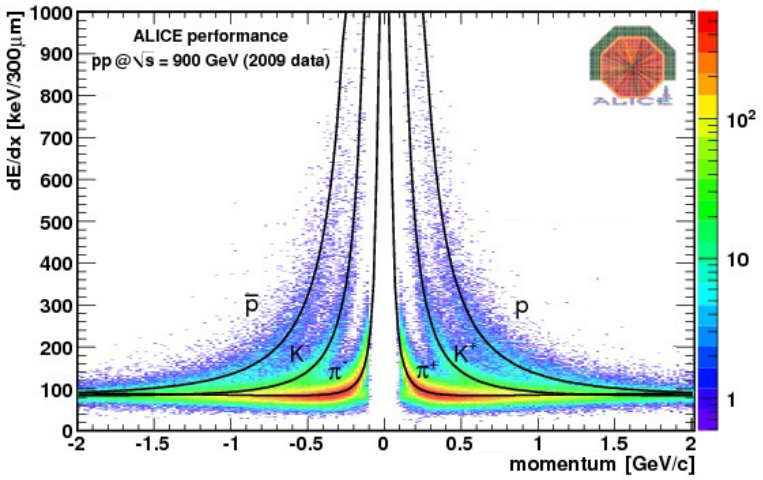

Figure 5: Energy Loss per Unit Length vs. Momentum for a Few Particles [9]

end plate. The x and y component of the electron position on this plate is equal to the x and y position of the charged particle at the time that it ionized the electrons. In addition, experimenters record the times that these electrons flew through the readout chambers, which gives us information about the z position of the charged particle at the time that it ionized the electrons. By keeping track of what times these electrons pass through the grid and which points on the grid they pass through, we can reconstruct the path that our particle of interest traced inside the TPC.

Since there are magnetic fields parallel to the length of the tube, our particle will trace out a curved path through the TPC. The curvature of the path gives us the momentum of the particle, and the number of electrons it ionizes from gas atoms gives us the energy loss per unit length dE/dx of the particle as it travels through the TPC. The cross section of the particle's interaction with gas atoms is dependent on the momentum of the particle and the intrinsic properties of the particle, such as its charge, mass and size. Thus, if we know the particle's momentum and we know its energy loss per unit length, we can identify the particle, as shown in Figure 5. This is the method of particle identification in ALICE.

1.3.2 The Time of Flight Detector

The Time of Flight (TOF) is another detector used in ALICE, shown in Figure 6 [10]. The purpose of the TOF is to measure charged particles' velocities. The TOF uses a triggered start-stop sequence to find the velocities of particles. The start signal is triggered when remnants of the lead nuclei flies through detectors at the ends of the tube. If the nuclei have

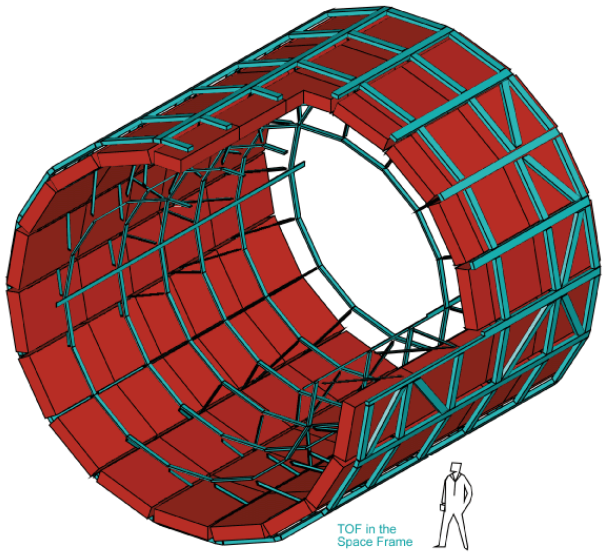

Figure 6: The ALICE Time of Flight Detector [10]

coincidence signals, meaning they triggered the start signal at the same time, then we know the collision happened at the center of the tube. We discard events which do not have this coincidence signal. The stop signal comes when a charged particle from the collision flies through the TOF tube itself, as pictured in Figure 6. The TOF records the time of the start signal and the time of the stop signal and, accounting for the known time it takes for the nuclei remnants to intersect the TOF detectors, these times give us the amount of time it took the particle to travel from the collision to the TOF detector. With positional data from the TPC, we are then able to calculate the velocity of the particle. The TOF has a time resolution of 100 picoseconds, which is the time it takes light to travel about 3 centimeters.

Since we can measure a particle's momentum with the TPC and its velocity with the TOF, we can then find its mass. This is a second method by which ALICE identifies charged particles.

1.3.3 Detector Observables

There are a few observables which are often used in particle physics. They are discussed here for reference. Firstly, the transverse momentum of a particle is the component of its momentum which is perpendicular to the beam axis (i.e. the z-axis). The symbol p_T is typically used to denote this quantity. Since the p_T includes only the x and y components of momentum,

we have that

$$p_T = \sqrt{p_x^2 + p_y^2}.$$

The rapidity of a particle, φ, is defined as the hyperbolic angle such that

$$\tanh \varphi = v/c$$

where v is the velocity of the particle. This quantity has the special property that it is additive across reference frames. That is, if φ_{XY} denotes the rapidity between reference frames X and Y, then $\varphi_{AC} = \varphi_{AB} + \varphi_{BC}$, assuming that the relative velocity between A and B and that between B and C are parallel. In particle physics, we also refer to y as the rapidity of a particle, where

$$\tanh y = v_z/c$$

letting v_z denote the component of the velocity along the beam axis. Thus, we have that

$$y = \tanh^{-1}(v_z/c) = \frac{1}{2} \ln \frac{1 + \beta_z}{1 - \beta_z}$$

where we have defined $\beta_z = v_z/c$. Below, we find that $p_z c = \beta_z E$ for a particle, hence we have that

$$y = \frac{1}{2} \ln \frac{E(1 + \beta_z)}{E(1 - \beta_z)} = \frac{1}{2} \ln \frac{E + p_z c}{E - p_z c}.$$

The pseudorapidity of a particle, η, is defined as

$$\eta = -\ln[\tan(\theta/2)]$$

where θ is the angle between the particle's velocity and the beam axis. This is the quantity commonly used to discuss a particle trajectory's polar angle.

2 Background

2.1 Special Relativity

When working with particles, one often is dealing with objects moving near the speed of light. Therefore, we introduce some of the ideas of special relativity here which are relevant to our study of particle physics.

We first define the relativistic quantities β and γ as

$$\beta \equiv v/c$$

$$\gamma \equiv \frac{1}{\sqrt{1 - \beta^2}}$$

where v is the speed of the object in question. Special relativity gives us a tool to move between different inertial reference frames. This tool is the

fundamental result of special relativity, not derived here, called the Lorentz transformation. It is written as

$$p'_{\parallel} = \gamma(p_{\parallel} + \beta E/c)$$

$$p'_{\perp} = p_{\perp}$$
$$E' = \gamma(E + \beta p_{\parallel} c)$$

Here β and γ correspond to the velocity of the first frame with respect to the second, primed momenta and energies are in the second frame while unprimed momenta and energies are in the first frame, $p_{\parallel}$ refers to the momentum component along the direction of the relative velocity of the frames, and $p_{\perp}$ refers to the momentum component perpendicular to this axis. We can use these relations to do calculations in the rest frame of a particle, which is often easier, and then boost those calculations into the lab frame.

A second standard result of special relativity that $p = \gamma m v = \gamma\beta mc$ and $E = \gamma mc^2$ where E is the energy, p is the momentum, and m is the mass of the particle. As pointed out above, this implies that $E\beta = pc$, or in particular, $E\beta_z = p_z c$. Using these facts, we have that

$$p^2c^2 + m^2c^4 = \frac{\beta^2 m^2 c^4}{1-\beta^2} + m^2c^4 = \frac{\beta^2 + 1 - \beta^2}{1-\beta^2} m^2c^4 = \frac{m^2c^4}{1-\beta^2} = (\gamma mc^2)^2 = E^2.$$

Thus, we find that

$$E^2 = (pc)^2 + (mc^2)^2.$$

This is the famous energy-momentum relation of special relativity. We will use this result to find the mass of particles from their energies and momenta.

2.2 Particle Decays

Consider a particle a which decays as $a \to bc$. By the laws of special relativity, this decay occurs the same way in all inertial reference frames, so we may examine the decay in the rest frame of particle a. In this frame, the momentum $\mathbf{p}_a$ of a is zero. By momentum conservation, we must have $\mathbf{p}_b + \mathbf{p}_c = 0$, so $\mathbf{p}_b = -\mathbf{p}_c$, i.e. b and c have equal but opposite momentum. In other words, the particles decay back-to-back. Since total momentum is zero in this frame, it is called the center-of-momentum (CM) frame.

Let $p := |\mathbf{p}_b| = |\mathbf{p}_c|$ be the common length momenta. Then by the energy-momentum relation, the energies of these particles are $E_b = \sqrt{p^2c^2 + m_b^2c^4}$ and $E_c = \sqrt{p^2c^2 + m_c^2c^4}$. Since $\mathbf{p}_a = 0$, we have $E_a = m_a c^2$. Invoking energy conservation, we obtain

$$m_a c^2 = \sqrt{p^2c^2 + m_b^2c^4} + \sqrt{p^2c^2 + m_c^2c^4}.$$

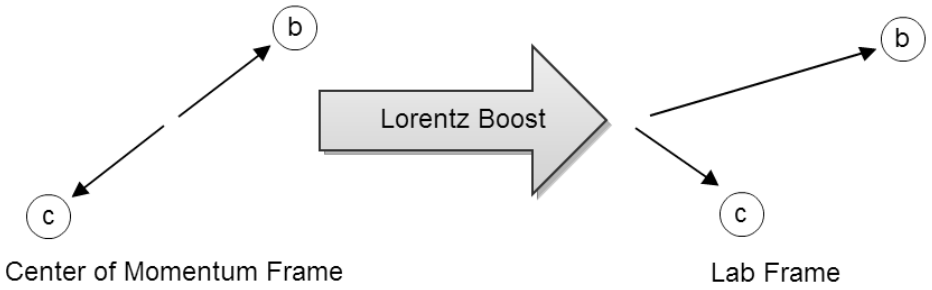

Figure 7: Lorentz Boost of a Decay

Thus, the magnitude of the daughter particles' momenta is uniquely determined in the CM frame. However, the direction in which they decay is not determined. Figure 7 shows a typical decay.

The figure demonstrates the fact that angles are not conserved in different frames. In this example, the momenta of particles b and c have an angle of 180° between them in the CM frame, but have an angle of less than 90° between them in the lab frame. Furthermore, if we vary the angle between the momentum of b and the boost axis, we vary the amount by which each momentum is boosted according to the Lorentz transformation. Thus, the angle between $\mathbf{p}_b$ and $\mathbf{p}_c$ in the lab frame depends on the direction in which the particles decay in the CM frame.

2.3 Resonance Particles

Consider a free particle, as described by quantum mechanics. In our initial naïve description, we solve the Schrödinger equation

$$i\hbar\frac{\partial}{\partial t}\Psi = \hat{H}\Psi$$

with $\hat{H} = -\frac{\hbar^2}{2m}\nabla^2$ for a free particle. Solving this equation, we obtain $\Psi(\mathbf{r},t) = Ae^{i(\mathbf{p}\cdot\mathbf{r}-E_0t)/\hbar}$ for a particle with momentum $\mathbf{p}$ and energy E_0, and where A is a constant. If $\psi(t)$ is the time component alone, we have $\psi(t) = \psi(0)e^{-iE_0t/\hbar}$. Of course, E_0 is a purely real number, hence $|\psi(t)|^2 = |\psi(0)|^2e^{-iE_0t/\hbar}e^{iE_0t/\hbar} = |\psi(0)|^2$, a constant. In other words, this model predicts no particle decays, something which is obviously incorrect. To correct for this, we introduce an imaginary component to the energy, so we have $E_0 \mapsto E_0 - i\Gamma/2$, where Γ is a real number. Plugging this in, we obtain $\psi(t) = \psi(0)e^{-\Gamma t/2\hbar - iE_0t/\hbar}$. Thus,

$$|\psi(t)|^2 = |\psi(0)|^2|e^{-\Gamma t/2\hbar}|^2|e^{-iE_0t/\hbar}|^2 = |\psi(0)|^2e^{-\Gamma t/\hbar}$$

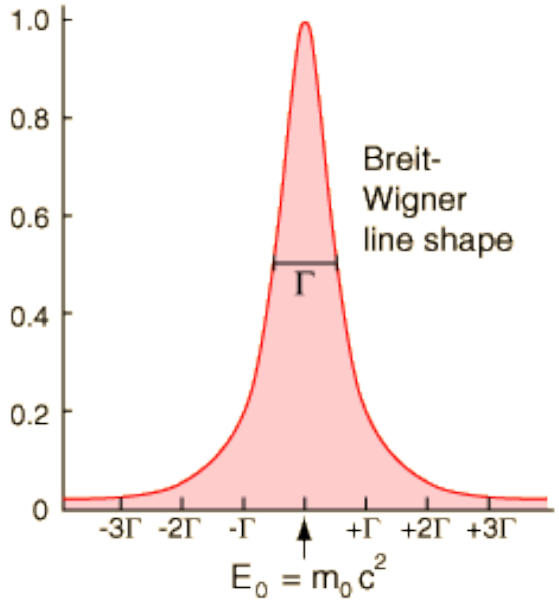

Figure 8: The Breit-Wigner Distribution [11]

so the particle's amplitude goes as $e^{-\Gamma t/\hbar}$, indicating that it decays. In fact, we define the lifetime of the particle τ such that it decays as $e^{-t/\tau}$, hence we have $\Gamma = \hbar/\tau$.

Now, consider the energy spectrum of such a particle. To analyze the spectrum, we take the Fourier transform of $\psi(t)$. We have

$$\phi(\omega) = \int_{-\infty}^{\infty} \psi(t) e^{i\omega t} dt$$

where $\omega = E/\hbar$. Integrating and substituting $\omega = E/\hbar$, we obtain

$$\phi(E) = \psi(0) \frac{1}{\Gamma/2\hbar + i(E_0 - E)/\hbar}.$$

We now normalize the wave function by setting $\int_0^{\infty} \phi^*(E)\phi(E)dE = 1$. Calculating the integral, we get $|\psi(0)|^2 = \Gamma/\hbar^2 2\pi$, so

$$\phi(E) = \sqrt{\frac{\Gamma}{2\pi}} \frac{1}{\Gamma/2 + i(E_0 - E)}.$$

The probability density $P(E)$ describing the energy distribution of this particle is then

$$P(E) = |\phi(E)|^2 = \frac{\Gamma}{2\pi} \frac{1}{(E - E_0)^2 + (\Gamma/2)^2}.$$

The is the Breit-Wigner distribution, displayed in Figure 8. The distribution has a width to it, determined by Γ. Thus, particles with finite lifetimes, and thus nonzero widths Γ, do not have definite masses.

Particles with relatively long lifetimes, such as the π^0, have small widths and thus their spread in mass is very small. In many cases, the width is indeed smaller than the experimental error made when measuring them in the first place, and thus the Breit-Wigner shape of the particle is not seen at all. Particles with shorter lifetimes, such as the Δ^0, have broad mass spectra and thus the width Γ of the particle is directly measurable.

3 Simulating the Δ^0 Resonance

3.1 HIJING

To analyze heavy ion interactions, we simulate collisions and examine the simulated detector responses. The tool we use to accomplish this is called the Heavy Ion Jet INteraction Generator, or HIJING [12]. The HIJING software simulates the scattering of several quarks off of one another within a heavy ion collision. Thus, it takes a first principles approach to predicting the nature of the QGP. It successfully simulates such phenomena as jet production (i.e. the tendency for many particles to travel in about the same direction at high momentum due to hard scattering of quarks) and QGP medium interaction with particles and jets (to the best of our current knowledge). Thus, it allows us to look inside the reaction as it unfolds and directly examine illusive particles such as the Δ^0 resonance. By examining these simulated particles, we can then make predictions about the nature and effects of these particles in actual experiments.

The AliRoot framework includes the HIJING software as a series of classes. In particular, the AliGenHijing class is used to generate collision simulations. The user sets the center-of-momentum energy, the reference frame, the colliding particles and other variables relevant to the collision. After the simulation is complete, the relevant information about each particle which is produced directly or indirectly from the collision is saved in a TParticle object. The TParticle objects are then entered into a stack which is saved in a ROOT file for later access.

Each collision is saved as an "event" in the ROOT file. Each event includes its collision's particle stack. Thus, when we access the file for further analysis, it is easy to evaluate every particle from every collision. We simply load up each event and iterate through the event's stack. This structure greatly simplifies the task of analyzing a particular particle over many collisions.

The code used to produce and save simulated collisions can be found in appendix A.

3.2 Invariant Mass Distribution

One of the most important ways we identify resonance particles is via their reconstructed invariant mass distributions. To find this distribution, we use events simulated with HIJING as discussed above. These events are stored in a number of different files, so our analysis program begins (after defining some variables to be used throughout the program) by looping through the files. Each file contains dozens of events, so we next loop over the stored events. For each event, we loop over the particles produced in the event. In this way, we can examine each particle of each event one at a time.

To represent the capabilities of the detectors used in ALICE, we make a pseudorapidity cut. In this case, we demand that our particles have a pseudorapidity η such that $|\eta| < 0.9$. This corresponds to particles whose direction of motion is at least $45°$ from the z-axis. This is a quality selection cut and is necessary to guarantee that our particles could have been seen by the ALICE detectors [10].

Next, we select all of the remaining particles which are Δ^0 resonances. For each Δ^0, we identify the particles into which it decays. The Δ particles decay into a nucleon and a pion, so in our case we have

$$\Delta^0 \to n\pi^0 \text{ or } \Delta^0 \to p\pi^-.$$

In the former case, both decay products are electrically neutral, and so we can detect neither of them. Therefore, we only examine Δ^0 resonances which decay to $p + \pi^-$. In this case, we store the information about the p and π^- daughters in a list to be examined later.

After we are done looping through the events in each file, we are ready to begin our calculation of the invariant mass distribution. We iterate over our list of daughter particles of Δ^0 decays. For each decay pair, we add the momenta and energies of the particles together. By momentum and energy conservation, this total momentum and energy must be equal to the original momentum and energy of the Δ^0. We then use the energy-momentum relation

$$E^2 = (mc^2)^2 + (pc)^2$$

to find the invariant mass of the Δ^0. The mass obtained for each decay pair is then entered in a histogram. The program described here can be found in appendix B.

Since resonance particles such as the Δ^0 have extremely short lifetimes, they have a noticeable width Γ to their mass, as shown in Figure 9. Therefore we expect repeated measurements of the Δ^0 mass to accumulate in a Breit-Wigner distribution, as discussed in Section 2.3. In this example, the Breit-Wigner fit produced a mean of 1.2340 ± 0.0008 GeV/c^2 and a width of 106 ± 2 MeV/c^2. The Particle Data Group (PDG) has as a standard that the Δ^0 mass is between 1.230 and 1.234 GeV/c^2 and the width is between 114 and 120 MeV/c^2. Thus, our mass measurement is correct, but our width measurement is a bit low in this simulation.

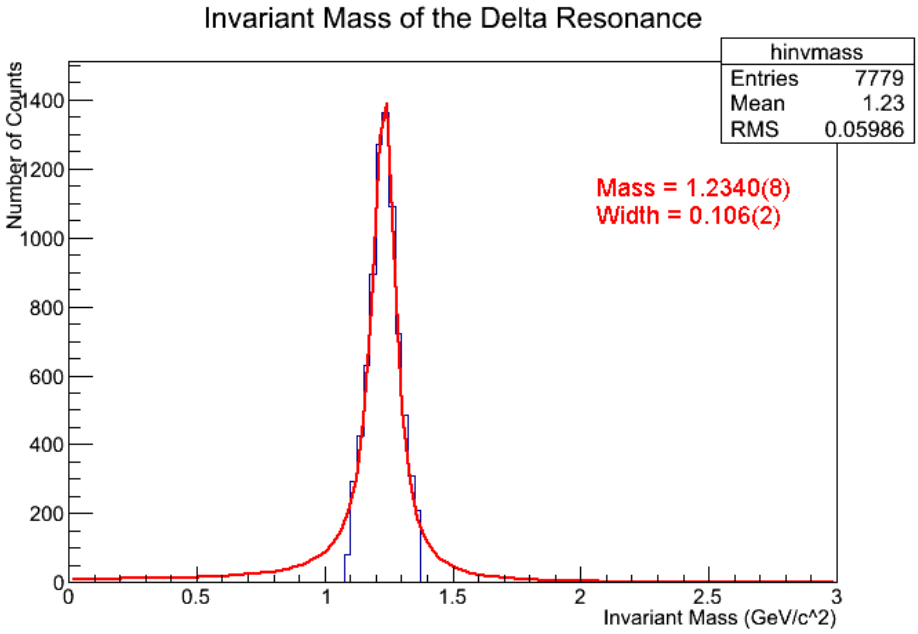

Figure 9: A typical invariant mass histogram of the delta resonance.

4 Particle Misidentification

When analyzing a particle collision, it is necessary to identify the particles produced in the interaction. Using the ALICE TPC detector (as discussed in Section 1.3 above), we can find the momentum p and energy loss per unit length dE/dx of any electrically charged particle which survives long enough to be seen by the TPC. As we discussed above, this gives us a way to identify charged particles.

However, it is not always easy to differentiate between particles using this method. As shown in Figure 5, the dE/dx values of different particles get close together as their momentum increases. Thus, it is the case that at high momenta, we may identify a π^+ as a p, or a K^+ as a π^+, etc. This causes a problem when we want to study high energy resonance particles, such as the Δ^0. We identify a Δ^0 by its decay products, and its most common decay to charged particles is $\Delta^0 \to p\pi^-$, as discussed above. We also know that K^0_S commonly decays via $K^0_S \to \pi^+\pi^-$. Thus, if we correctly identify the π^- but misidentify the π^+ as a p, then we would reconstruct a Δ^0 from the decay products of a K^0_S. Therefore, we would over count the number of Δ^0 produced, and since the π^+ and π^- did not actually come from a Δ^0, our reconstructed invariant mass distribution would be skewed. It is important to understand the contributions of misidentified particles to measured distributions of the Δ^0 so that we may produce a cleaner Δ^0

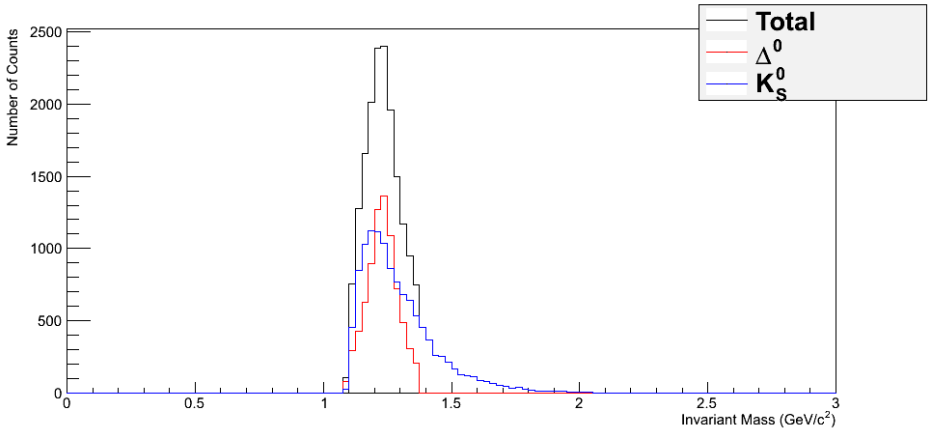

Figure 10: Δ^0 Distribution and 5% of K^0_S Misidentified Distribution

signal.

4.1 Simulating Misidentification

To study particle misidentification, we use a modified version of our invariant mass program. Say that we are looking at the misidentification of the particle A. Then instead of picking out decay products of the Δ^0, we select decay products of the A. As before, we loop through the events in each file, and for each event, we store the decay products of the A particles in lists for later analysis. After looping through all events, we then find the invariant mass distribution by misidentifying one of the particle's decay products and reconstructing. Say that we are misidentifying a π^+ as a p in the decay $A \to \pi^+\pi^-$. Then we use the original π^+ momentum for our misidentified particle, but instead of using its energy, we calculate a misidentified energy by substituting the p mass and using the energy-momentum relation $E^2 = (pc)^2 + (mc^2)^2$. We then combine this misidentified particle with the correctly identified π^- to get the invariant mass of the misidentified mother particle.

4.1.1 K^0_S Misidentification

The K^0_S commonly decays as $K^0_S \to \pi^+\pi^-$. Thus, it can be mistaken for a Δ^0 if we misidentify the π^+ as a p. Because there are many more K^0_S particles than Δ^0 particles produced in an event, we have taken only 5% of the K^0_S distribution. This misidentified distribution is shown in Figure 10, with the Δ^0 distribution and total distribution included.

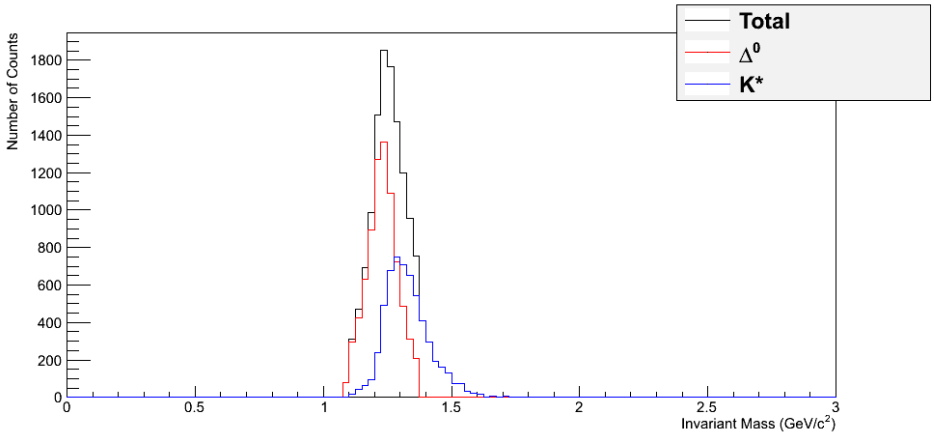

Figure 11: Δ^0 Distribution and 5% of K^* Misidentified Distribution

4.1.2 $K^*(892)$ Misidentification

The $K^*(892)$ is an excited state of the K^0. It commonly decays as $K^* \rightarrow K^+\pi^-$. If the K^+ is mistaken for a p, then the K^* is misidentified as a Δ^0. Because there are many more K^* particles than Δ^0 particles produced in an event, we have taken only 5% of the K^* distribution. This misidentified distribution is shown in Figure 11, with the Δ^0 distribution and total distribution included.

4.1.3 $\rho(770)$ Misidentification

Like the K^0_S, the $\rho(770)$ commonly decays to $\pi^+\pi^-$, so if we mistake the π^+ for a proton, then the ρ is misidentified as a Δ^0. Because there are many more ρ particles than Δ^0 particles produced in an event, we have taken only 5% of the ρ distribution. This misidentified distribution is shown in Figure 12, with the Δ^0 distribution and total distribution included.

4.1.4 $\omega(782)$ Misidentification

The $\omega(782)$ commonly decays as $\omega \rightarrow \pi^+\pi^-\pi^0$. Therefore we can misidentify it as a Δ^0 if we mistake the π^+ for a p and ignore the π^0. Unfortunately, the ROOT class TParticle does not support particles with more than two decay products. By default, it only keeps track of the first two daughter particles. To work around this issue, we first take all of the ω particles which have a charged π as one of their first two daughters. For these, the software stores the two daughters in the decay lists without regard to which π has which charge. Since all of the π are nearly degenerate in mass, the dynamics of the daughters are equal to one another on average. Thus, we

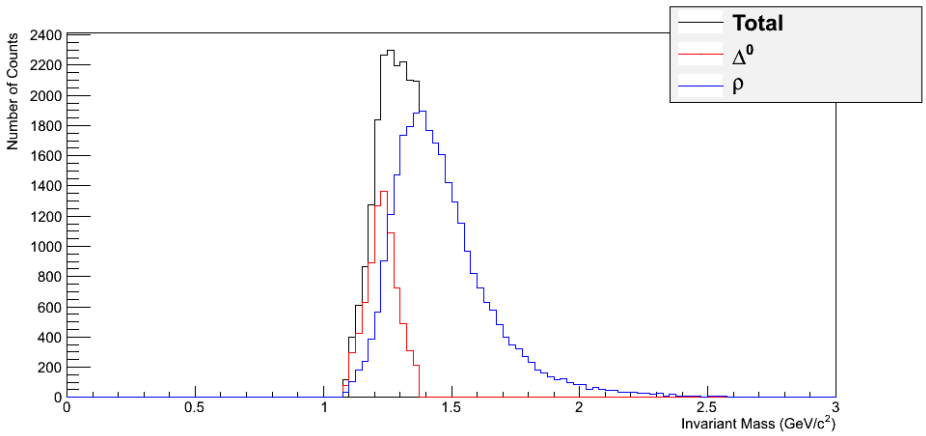

Figure 12: Δ^0 Distribution and 5% of ρ Misidentified Distribution

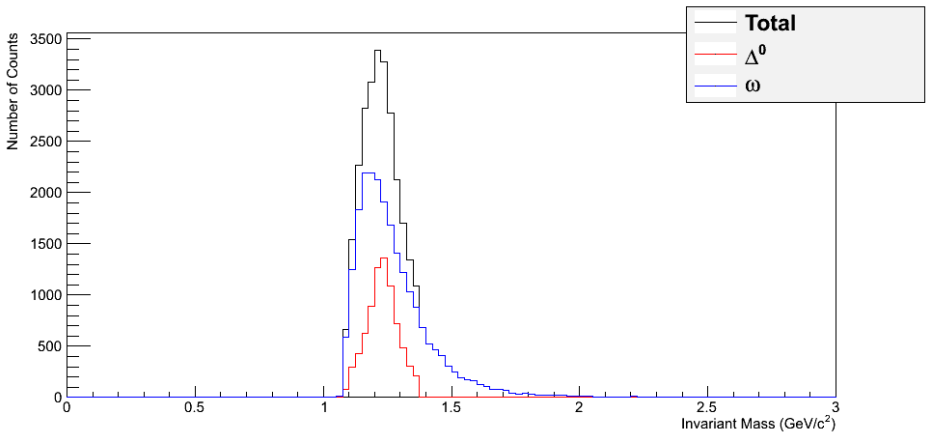

Figure 13: Δ^0 Distribution and 5% of ω Misidentified Distribution

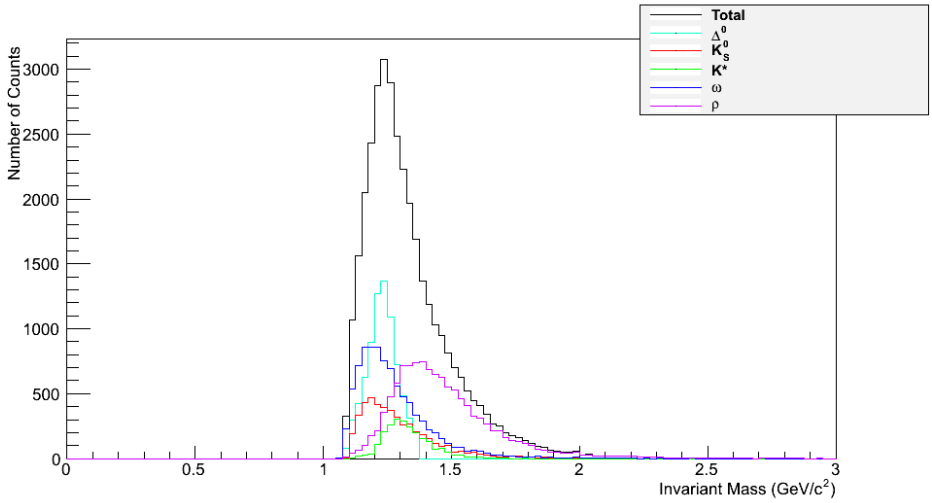

Figure 14: Δ^0 Distribution and 2% of Each Misidentified Distribution

simply assign one of the π daughters the p mass and combine it with the other π daughter to simulate the ω misidentification. Our results are the same as we would have obtained had we assigned the π^+ daughter the p mass and recombined it with the π^- daughter.

Because there are many more ω particles than Δ^0 particles produced in an event, we have taken only 5% of the ω distribution. This misidentified distribution is shown in Figure 13, with the Δ^0 distribution and total distribution included.

4.1.5 Total Misidentification

A summary plot of all misidentification distributions is shown in Figure 14. We have also included the Δ^0 distribution and the sum total of all of these distributions. Here we have taken only 2% of each distribution since the total distribution includes every misidentified particle we have analyzed so far, and any bigger of a contamination would completely drown out the Δ^0 signal.

5 Momentum Dependence

5.1 Invariant Mass Spectrum Shape

In the above plots, we have taken data from the entire p_T range of the mother particle. For the Δ^0 signal, it does not change anything to view its distribution in some smaller p_T range since it has the same mass and

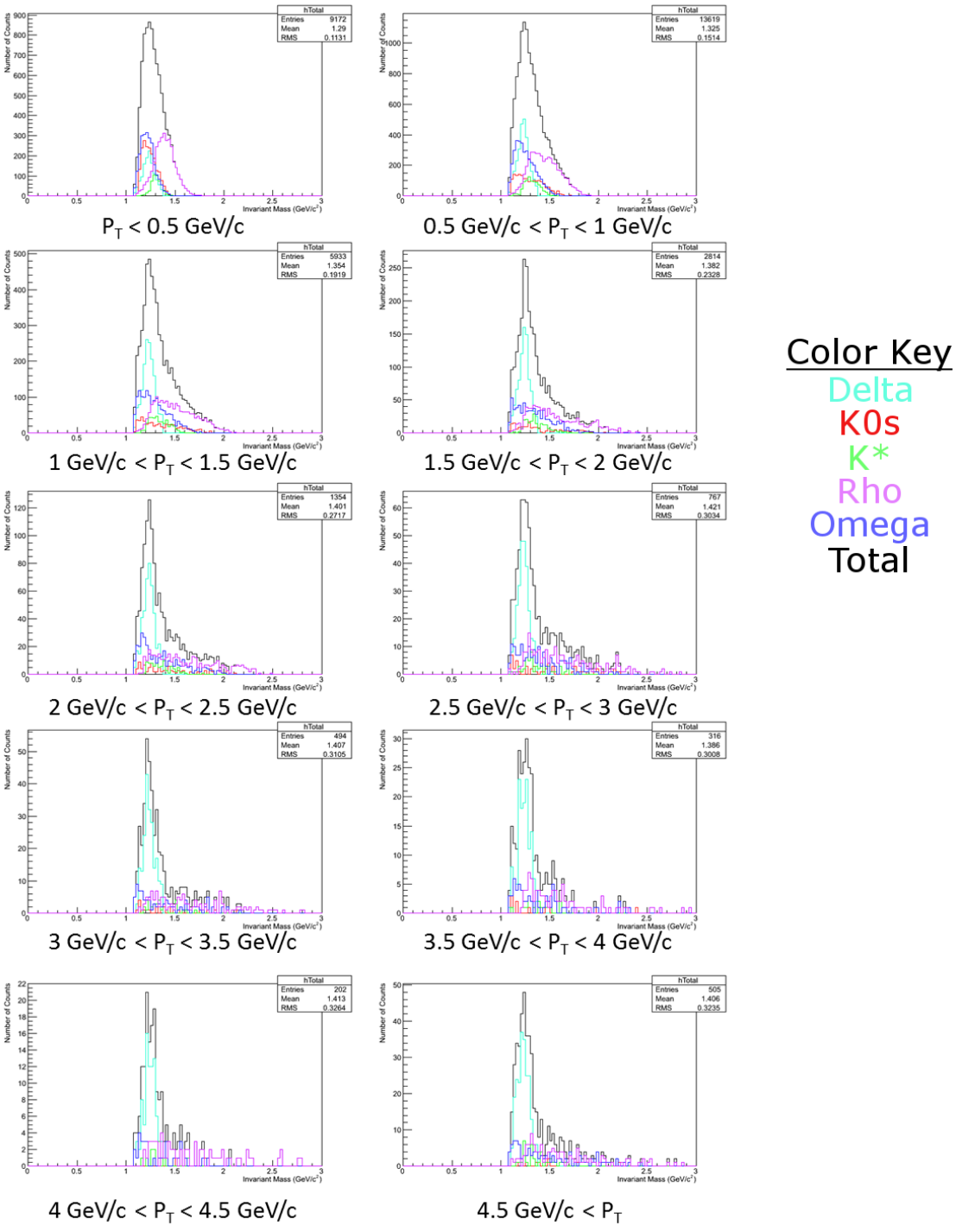

Figure 15: Invariant Mass Distribution of the Δ^0 and 2% of the Distributions of the Misidentified Particles in Various p_T Ranges

width regardless of its momentum. The misidentified spectra, however, are not determined by intrinsic properties of the misidentified particle, so their shape can change in different p_T regions.

To analyze how the shape changes, it is necessary to create plots of the invariant mass distributions of the misidentified particles in different p_T ranges. To this end, while finding the misidentified distributions in the first place, we not only store the invariant mass calculations, but also the p_T of the mother particle for each calculation. Thus, every entry in an invariant mass spectrum has an associated p_T value. Later, we loop through these mass, p_T pairs with a momentum cut in mind. If the p_T value is within the bounds of the cut, we enter the mass value into our distribution. This is a convenient method to quickly build the invariant mass spectra of misidentified particles in various p_T regions. The results of this analysis are shown in Figure 15, with Δ^0 and total distributions included. Once again, we have used only 2% of the misidentified distributions to ensure that the Δ^0 signal can be seen over the misidentified background.

At low momentum (less than 0.5 GeV/c), each of the distributions looks very much like a Breit-Wigner hump. Except for the ρ, all humps peak near the Δ^0 mass of 1.232 GeV/c^2 and do not trail off very much, so they may be difficult to distinguish from the real Δ^0 signal at this momentum value.

At somewhat higher momentum (starting at 1 GeV/c or so) each of the distributions has developed a long tail in the higher invariant mass region. Since the real Δ^0 invariant mass spectrum has no such tail, this is a shape unique to the misidentified particles' distributions. With some knowledge of the expected shape of the misidentified distributions, we can use this to estimate the distribution of misidentified particles in an experimental distribution. More is said on this in the Conclusion.

At high momentum (2 GeV/c and higher), the tail of each individual distribution is very long. In this momentum region, any one misidentified particle's tail would likely be obvious in an experimental Δ^0 invariant mass spectrum.

5.2 Peak Location

If the peak of a misidentified distribution is far enough from the Δ^0 mass, we may be able to identify it in a mass spectrum from an experiment. This will assist us in guessing the spectrum of misidentified particles. To see in which p_T ranges this occurs for each misidentified particle, we run through each of the spectra found above and look for the bin in the histogram with the greatest number of counts. This bin is the peak of the spectrum. We then plot these peaks in the graph shown in Figure 16. Note that the horizontal error bars represent the p_T range over which the peak was found, while the vertical error bars correspond to the bin size used while finding the peak.

Looking at the graph, we notice a few features of the invariant mass

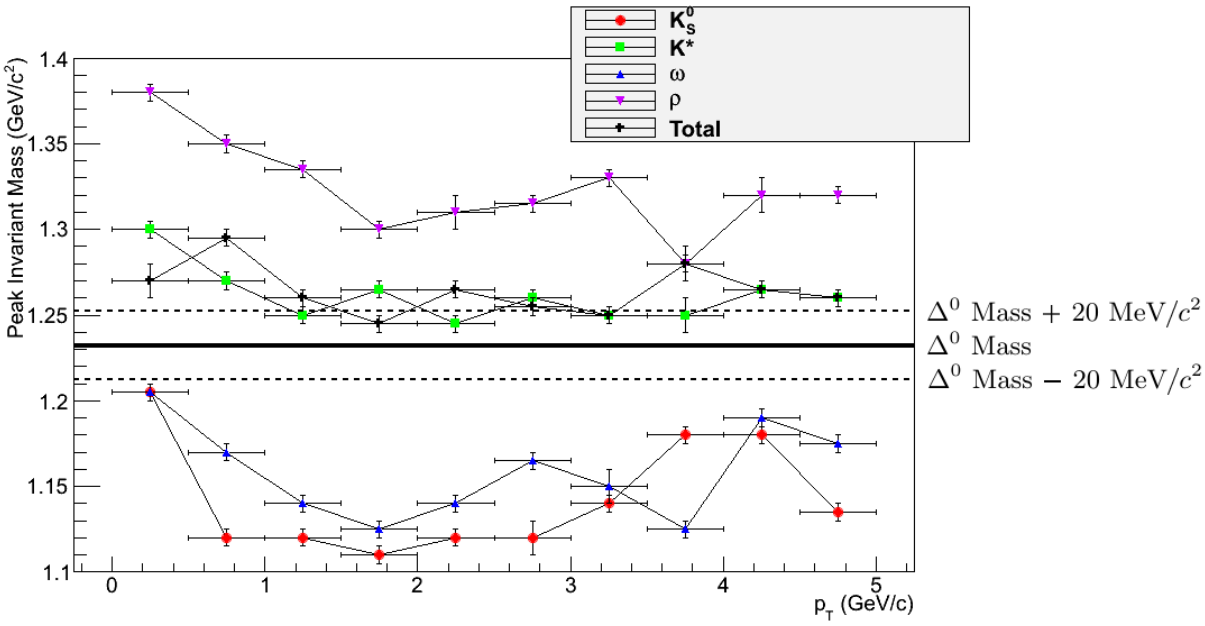

Figure 16: Peaks of Invariant Mass Spectra in Various p_T Ranges

distributions. Firstly, the K^0_S and ω distributions' peaks are only near the Δ^0 mass at low p_T, namely for $p_T < 0.5$ GeV/c. Thus, if we look at the Δ^0 distribution for higher p_T, then we should expect to see the peaks of the K^0_S and ω misidentified distributions outside of the Δ^0 peak. The ρ distribution never peaks near the Δ^0 mass. Thus, we should always expect to be able find its peak in a Δ^0 invariant mass distribution. The K^* peak is very often near the Δ^0 mass, so we should expect to have trouble identifying its peak in a Δ^0 distribution. For this reason, we require a very low contamination from K^* misidentification if we are to accurately analyze the Δ^0 signal in an experiment. In other words, we must be able to distinguish between K^+ and p with great accuracy. Finally, the total background peak appears to be near the Δ^0 mass for momenta between 1 and 3.5 GeV/c, so we should only expect to pick out its peak in the low momentum and very high momentum ranges. This, however, is based on a contamination from each misidentified particle exactly proportional to the number of that particle produced in a collision. If we could decrease the K^* contamination, we would expect to see the total misidentification peak shift away from the Δ^0 mass in the mid momentum range. The data of Figure 16 are listed in a table in Appendix C.

6 Conclusion

By simulating the invariant mass distributions of misidentified particles, we found the shape of the misidentified particles' contributions to the mass spectrum of the Δ^0 in ALICE. Furthermore, we observed the way this shape changes in different p_T ranges and where the peaks of these distributions were located as we varied p_T.

The next step would be to begin finding functions that match the misidentified spectra in each p_T range. Once we have a working model for each distribution, we can now begin to find these misidentified spectra in experimental distributions of the Δ^0 invariant mass. After picking a particular p_T range, we have an expectation of where each peak in the misidentified distributions should be and what the shape of those distributions should look like. Thus, we can fit a sum of these models to our data. We can then measure the number of misidentified K^* particles in our distribution, for instance. Furthermore, by understanding the misidentified background to our signal, we can subtract it out, leaving us with a cleaner Δ^0 distribution. Cleaner measurements of the Δ^0 then give us more accurate information about the QGP.

We note here that a better method may yield cleaner and more useful results in the peak analysis above. Rather than simply taking the maximum bin of each distribution, we should have fit a Gaussian curve to the part of each distribution containing the peak. This method is much less sensitive to random fluctuations in the distributions and would likely give more accurate calculations of the peak of each distribution. Future experimenters should make use of this method.

A fastGen.C

```
void fastGen(Int_t nev = 100, char* filename = "galice1/galice.root")
{

    cout << nev << endl;
    cout << filename << endl;

//  Runloader
  gRandom->SetSeed(0);//put 0 to use system time
  gSystem->SetIncludePath("-I$ROOTSYS/include -I$ALICE_ROOT/include -I$ALICE_ROOT");
  gSystem->Load("libhijing.so");
  gSystem->Load("libTHijing.so");      // AliGenHijing is defined here
  gSystem->Load("liblhapdf.so");       // Parton density functions
  gSystem->Load("libEGPythia6.so");    // TGenerator interface
  gSystem->Load("libpythia6.so");      // Pythia
  gSystem->Load("libAliPythia6.so");   // ALICE specific implementations
```

```
  AliRunLoader* rl = AliRunLoader::Open(filename, "FASTRUN", "recreate");

  rl->SetCompressionLevel(2);
  rl->SetNumberOfEventsPerFile(nev);
  rl->LoadKinematics("RECREATE");
  rl->MakeTree("E");
  gAlice->SetRunLoader(rl);

//  Create stack
  rl->MakeStack();
  AliStack* stack = rl->Stack();

//  Header
  AliHeader* header = rl->GetHeader();

//  Create and Initialize Generator
  AliGenHijing *gener = new AliGenHijing(-1);
// centre of mass energy
  gener->SetEnergyCMS(5500.);
//reference frame
  gener->SetReferenceFrame("CMS");
// projectile
  gener->SetProjectile("A", 208, 82);
  gener->SetTarget    ("A", 208, 82);
// tell hijing to keep the full parent child chain
  gener->KeepFullEvent();
// enable jet quenching
  gener->SetJetQuenching(0); //RHIC quenching
// enable shadowing
  gener->SetShadowing(1);
// neutral pion and heavy particle decays switched off
  gener->SetDecaysOff(0);
// Don't track spectators
  gener->SetSpectators(0);
// kinematic selection
  gener->SetSelectAll(0);

  gener->SetImpactParameterRange(0.0,4.8);

   //   Initialize generator
  gener->Init();
  gener->SetStack(stack);

//
//                         Event Loop
//
```

```
  Int_t iev;

  for (iev = 0; iev < nev; iev++) {
    Printf(Form(" Event number %d", iev));

//  Initialize event
    header->Reset(0,iev);
    rl->SetEventNumber(iev);
    stack->Reset();
    rl->MakeTree("K");

//  Generate event
    gener->Generate();

//  Finish event
    header->SetNprimary(stack->GetNprimary());
    header->SetNtrack(stack->GetNtrack());

//  I/O
    stack->FinishEvent();
    header->SetStack(stack);
    rl->TreeE()->Fill();
    rl->WriteKinematics("OVERWRITE");

    } // event loop

//  Termination

//  Generator
  gener->FinishRun();

//  Write file
  rl->WriteHeader("OVERWRITE");
  gener->Write();
  rl->Write();
}
```

B deltaInvMass.C

```
#include "/Volumes/MacintoshHD3/agrounds/programs/hijing/PDGCodes.h"
#include "/Volumes/MacintoshHD3/agrounds/programs/hijing/DoubleWrap.h"


void deltaInvMass(const char *ex = "001",
                  const char *outputFileName = "./data_invmass/deltaInvMass.root") {
```

```
// Dynamically link some shared libs

  if (gClassTable->GetID("AliRun") < 0) {
  gROOT->LoadMacro("loadlibs.C");
  loadlibs();
  }

  gSystem->SetIncludePath("-I$ROOTSYS/include -I$ALICE_ROOT/include -I$ALICE_ROOT");
  gSystem->Load("libhijing.so");
  gSystem->Load("libTHijing.so");    // AliGenHijing is defined here
  gSystem->Load("liblhapdf.so");     // Parton density functions
  gSystem->Load("libEGPythia6.so");    // TGenerator interface
  gSystem->Load("libpythia6.so");    // Pythia
  gSystem->Load("libAliPythia6.so");  // ALICE specific implementations


  Int_t fileok =0;
  Int_t Nevents =0;



  Int_t mpart;                    //gMC->TrackPid()


  Double_t Pt;


  TObjArray *pos = new TObjArray();
  TObjArray *neg = new TObjArray();

  TObjArray *decay1 = new TObjArray(); //proton
  TObjArray *decay2 = new TObjArray(); //pion


  const Int_t hinvmassLow  = 0;
  const Int_t hinvmassHigh = 3;
  const Int_t hinvmassNum  = (hinvmassHigh - hinvmassLow) / 0.025;

  TH1F *hinvmass     =  new TH1F("hinvmass", "Invariant Mass of the Delta Resonance",
                                 hinvmassNum, hinvmassLow, hinvmassHigh);
  hinvmass->GetXaxis()->SetTitle("Invariant Mass (GeV/c^2)");
  hinvmass->GetYaxis()->SetTitle("Number of Counts");

  TH1F *hNev = new TH1F("hNev","Nev.",10,0,10);
```

```
  std::vector<Double_t> massList, ptList;

  char* directory = "/Volumes/MacintoshHD3/agrounds/programs/hijing/galice/";
  void *pDir = gSystem->OpenDirectory(directory);
  const char* fileName(0);

  AliRunLoader* rl = new  AliRunLoader();


  // loop through folders holding event files
  while((fileName = gSystem->GetDirEntry(pDir))) {
    fileok = 0;
    const TString file(fileName);

    if(file.Contains("galice")) {
      cout << " file ok "<<endl;
      fileok = 1;
      const TString file2 = "/Volumes/MacintoshHD3/agrounds/programs/hijing/galice/"
                            + file + "/galice.root";

      // Connect the Root Galice file containing Geometry, Kine and Hits
      AliRunLoader* rl = 0x0;
      rl = AliRunLoader::Open(file2, AliConfig::GetDefaultEventFolderName(),
"read");
      if (rl == 0x0) {
        delete rl;
        continue;
      }

      Int_t numOfevents = rl->GetNumberOfEvents();



      //
      //   Loop over events
      //

      rl->LoadKinematics();
      rl->LoadHeader();

      for (Int_t nev=0; nev<numOfevents;  nev++) {
        hNev->Fill(1);
        cout<< " ----------event----------"<<Nevents++<<endl;

        Printf(Form(" Event number %d", nev));
```

```
  rl->GetEvent(nev);
        AliStack* stack = rl->Stack();
  Int_t npart = stack->GetNprimary();


  //
  // Loop over primary particles
  //

  cout << " number of particles " << npart<<endl;
  for (Int_t part=0; part< npart; part++) {
    TParticle *MPart = stack->Particle(part);

    mpart  = MPart->GetPdgCode();
    Pt = MPart->Pt();

    Double_t eta = MPart->Eta();

    // make lists for inv mass
    if (abs (eta) < 0.9) {
      if (mpart == DELTA0 && MPart->GetNDaughters() >= 2) {
        TParticle *child1 = stack->Particle(MPart->GetDaughter(0));
        TParticle *child2 = stack->Particle(MPart->GetDaughter(1));

        if (child1->GetPdgCode() == PROTON && child2->GetPdgCode() == PIm1) {
          decay1->AddLast(new TParticle(*child1));
          decay2->AddLast(new TParticle(*child2));
          ptList.push_back(Pt);
        }
        if (child2->GetPdgCode() == PROTON && child1->GetPdgCode() == PIm1) {
          decay1->AddLast(new TParticle(*child2));
          decay2->AddLast(new TParticle(*child1));
          ptList.push_back(Pt);
        }
      }
    }


  } //prim loop




} // event loop
```

```
    if(fileok ==1) {
      delete rl;
    }

  } // if loop

} // file loop


//find delta mass distribution

TParticle *child1, *child2;
const Int_t numDecay = decay1->GetEntries();

cout << "numDecay = " << numDecay << endl;

for (Int_t i = 0; i < numDecay; ++i) {
  child1 = (TParticle *) decay1->At(i);
  child2 = (TParticle *) decay2->At(i);

  TLorentzVector mom(child1->Px() + child2->Px(), child1->Py() + child2->Py(),
                     child1->Pz() + child2->Pz(),
                     child1->Energy() + child2->Energy());
  hinvmass->Fill(mom.M());
  massList.push_back(mom.M());
}

const Int_t arrDim = numDecay;

Double_t massArr[arrDim];
Double_t ptArr[arrDim];

//create TTree for writing data
TTree* tree = new TTree("tree", "Mass and Pt Lists");
tree->Branch("numDecay", &numDecay, "numDecay/I");
tree->Branch("massArr", massArr, "massArr[numDecay]/D");
tree->Branch("ptArr", ptArr, "ptArr[numDecay]/D");

for (Int_t i = 0; i < numDecay; ++i) {
  massArr[i] = massList[i];
  ptArr[i] = ptList[i];
}

tree->Fill();
```

```
  TFile *outfile = new TFile(outputFileName,"RECREATE","Histofile");

  outfile->cd();

  hNev->Write();

  hinvmass->Write();

  tree->Write();

  outfile->Close();
}
```

C Figure 16 Data

The K_S^0 data:

p_T Range (GeV/c)	Peak (GeV/c^2)	Bin Size (GeV/c^2)
$0 < p_T < 0.5$	1.205	0.005
$0.5 < p_T < 1$	1.12	0.005
$1 < p_T < 1.5$	1.12	0.005
$1.5 < p_T < 2$	1.11	0.005
$2 < p_T < 2.5$	1.12	0.005
$2.5 < p_T < 3$	1.12	0.01
$3 < p_T < 3.5$	1.14	0.005
$3.5 < p_T < 4$	1.18	0.005
$4 < p_T < 4.5$	1.18	0.005
$4.5 < p_T$	1.135	0.005

The K^* data:

p_T Range (GeV/c)	Peak (GeV/c^2)	Bin Size (GeV/c^2)
$0 < p_T < 0.5$	1.3	0.005
$0.5 < p_T < 1$	1.27	0.005
$1 < p_T < 1.5$	1.25	0.005
$1.5 < p_T < 2$	1.265	0.005
$2 < p_T < 2.5$	1.245	0.005
$2.5 < p_T < 3$	1.26	0.005
$3 < p_T < 3.5$	1.25	0.005
$3.5 < p_T < 4$	1.25	0.01
$4 < p_T < 4.5$	1.265	0.005
$4.5 < p_T$	1.26	0.005

The ω data:

p_T Range (GeV/c)	Peak (GeV/c^2)	Bin Size (GeV/c^2)
$0 < p_T < 0.5$	1.205	0.005
$0.5 < p_T < 1$	1.17	0.005
$1 < p_T < 1.5$	1.14	0.005
$1.5 < p_T < 2$	1.125	0.005
$2 < p_T < 2.5$	1.14	0.005
$2.5 < p_T < 3$	1.165	0.005
$3 < p_T < 3.5$	1.15	0.01
$3.5 < p_T < 4$	1.125	0.005
$4 < p_T < 4.5$	1.19	0.005
$4.5 < p_T$	1.175	0.005

The ρ data:

p_T Range (GeV/c)	Peak (GeV/c^2)	Bin Size (GeV/c^2)
$0 < p_T < 0.5$	1.38	0.005
$0.5 < p_T < 1$	1.35	0.005
$1 < p_T < 1.5$	1.335	0.005
$1.5 < p_T < 2$	1.3	0.005
$2 < p_T < 2.5$	1.31	0.01
$2.5 < p_T < 3$	1.315	0.005
$3 < p_T < 3.5$	1.33	0.005
$3.5 < p_T < 4$	1.28	0.005
$4 < p_T < 4.5$	1.32	0.01
$4.5 < p_T$	1.32	0.005

The Total Distribution data:

p_T Range (GeV/c)	Peak (GeV/c^2)	Bin Size (GeV/c^2)
$0 < p_T < 0.5$	1.27	0.01
$0.5 < p_T < 1$	1.295	0.005
$1 < p_T < 1.5$	1.26	0.005
$1.5 < p_T < 2$	1.245	0.005
$2 < p_T < 2.5$	1.265	0.005
$2.5 < p_T < 3$	1.255	0.005
$3 < p_T < 3.5$	1.25	0.005
$3.5 < p_T < 4$	1.28	0.01
$4 < p_T < 4.5$	1.265	0.005
$4.5 < p_T$	1.26	0.005

References

[1] Nave, R. Color Force. Hyper Physics. Georgia State University. <http://hyperphysics.phy-astr.gsu.edu/hbase/forces/color.html>.

[2] Heavy-ion collisions, the quark-gluon plasma, and quantum chromodynamics. CERN Press Office. CERN. <http://press.web.cern.ch/backgrounders/heavy-ion-collisions-quark-gluon-plasma-and-quantum-chromodynamics>.

[3] Some results from the first two years of lead ion collisions. The ALICE Collaboration. CERN. 2012. <http://aliceinfo.cern.ch/Public/en/Chapter1/results.html>.

[4] Zakout, I. and Greiner C. The quark-gluon-plasma phase transition diagram, Hagedorn matter and quark-gluon liquid. 2010. arXiv:1002.3119 [nucl-th].

[5] Uwer, Ulrich. Elements of QCD - SU(3) Theory. Heidelberg University. <http://www.physi.uni-heidelberg.de/ uwer/lectures/ParticlePhysics/Vorlesung/Lect-5a.pdf>.

[6] J. Beringer et al. (Particle Data Group), Phys. Rev. D86, 010001 (2012).

[7] Nagel, Darragh E. The Delta: The First Pion Nucleon Resonance. Los Alamos National Laboratory. 1982. <http://www.osti.gov/accomplishments/documents/fullText/ACC0011.pdf>

[8] The ALICE Time Projection Chamber (TPC). The ALICE Collaboration. CERN. 2008. <http://aliceinfo.cern.ch/Public/en/Chapter2/Chap2_TPC.html>.

[9] Preghenella, Roberto. Particle Identification at the LHC with the ALICE Experiment. The ALICE Collaboration. 2010. Slide 7. <http://confs.obspm.fr/Blois2010/Preghenella.pdf>.

[10] The ALICE Time of Flight Detector. The ALICE Collaboration. CERN. 2008. <http://aliceinfo.cern.ch/Public/en/Chapter2/Chap2_TOF.html>.

[11] Nave, R. Particle lifetimes from the uncertainty principle. Hyper Physics. Georgia State University. <http://hyperphysics.phy-astr.gsu.edu/hbase/quantum/parlif.html>.

[12] Deng W., Wang X. and Xu, R. Hadron production in p+p, p+Pb, and Pb+Pb collisions with the HIJING 2.0 model at energies available at the CERN Large Hadron Collider. 2011. arXiv:1008.1841 [hep-ph].